Available online at www.sciencedirect.com
ScienceDirect
Ceramics International 37 (2011) 1427–1434
CERAMICS INTERNATIONAL
www.elsevier.com/locate/ceramint

Thermal shock resistance and fatigue of Zircon–Mullite composite materials

N.M. Rendtorff [a,b,c,*], L.B. Garrido [a,d], E.F. Aglietti [a,b,d]

[a] Centro de Tecnología de Recursos Minerales y Cerámica (CETMIC): (CIC-CONICET-CCT La Plata), Camino Centenario y 506, C.C.49 (B1897ZCA) M.B.Gonnet, Buenos Aires, Argentina
[b] Facultad de Ciencias Exactas - Universidad Nacional de La Plata, UNLP, Argentina
[c] CIC-PBA, Buenos Aires, Argentina
[d] CONICET, Buenos Aires, Argentina

Received 4 January 2011; received in revised form 24 January 2011; accepted 25 January 2011
Available online 1 February 2011

Abstract

Zircon–Mullite ($ZrSiO_4$–$3Al_2O_3{\cdot}2SiO_2$) composites are refractory materials widely employed in many industries. Thermal shock behaviour of these materials must be considered because it is sometimes its failure mechanism.

In this work both thermal shock resistance (TSR) and fatigue (TFR) of Zircon–Mullite composites with different compositions and microstructure configurations were experimentally evaluated by a non destructive measurement of the elastic modulus (E) and compared with the prediction made from the theoretical parameters (R, R''' and R_{ST}).

A typical solid brittle material behaviour was found; a simple mathematical expression facilitated the TFR analysis. Although the microstructural configurations studied differed, the experimental behaviour of this group of materials was almost equal. This fact was satisfactorily predicted by the theoretical parameters (R and R''') showing the importance and potential of the evaluation mechanical evaluation of the ceramic material that define these two parameters. On the other hand the slight difference evaluated in the TFR was correlated with the only parameter that takes into account the fracture toughness (R_{ST}) showing that the significance of this property in a more deep characterization of the ceramic materials.

Keywords: B. Composites; D. Mullite; Thermal shock and thermal fatigue; Zircon

1. Introduction

Many ceramics and refractory materials are submitted to severe thermomechanical stresses during their installation or service. A good behaviour of the material to a sudden temperature change is known as good thermal shock resistance.

Ceramic materials are polycrystalline and the initiation of a crack occurs easily, the fracture mechanisms are closely related to the microstructure, such as pores or cracks and grain boundaries. The microstructure is a characteristic that should be controlled in order to decrease the damage due to thermal shocks.

Zircon ($ZrSiO_4$) is a good refractory material because it does not undergo any structural transformation until its dissociation at about 1450 to 1700 °C, depending on the present impurities. It exhibits many attractive properties such as excellent chemical stability and, coupled with a very low thermal expansion coefficient (4.1×10^{-6} °C^{-1} from room temperature to 1400 °C) and low heat conductivity coefficient (5.1 W/m °C at room temperature and 3.5 W/m °C at 1000 °C). These properties, together with good mechanical properties make this material a potential candidate as a useful structural ceramic. These materials are widely used mainly in the glass and molten salts industries [1–5]. Thermal shock resistance is a behaviour that affects the performance of Zircon ceramics due to the important extent of damage or degradation of the material. Hence Zircon based dense materials degradation by a thermal shock condition is sometimes the limiting property for its applications.

On the other hand Mullite ($3Al_2O_3{\cdot}2SiO_2$) ceramics have, had and will continue to have a significant role in the development of traditional and advanced ceramics [6].

Ceramic–ceramic composites can achieve a better performance than materials processed from a single phase. Several

* Corresponding author at: Centro de Tecnología de Recursos Minerales y Cerámica (CETMIC): (CIC-CONICET-CCT La Plata), Camino Centenario y 506, C.C.49 (B1897ZCA) M.B.Gonnet, Buenos Aires, Argentina.
Tel.: +54 2214840247; fax: +54 2214710075.
E-mail address: rendtorff@cetmic.unlp.edu.ar (N.M. Rendtorff).

0272-8842/$36.00
doi:10.1016/j.ceramint.2011.01.004

studies had been made in Zircon based composites with different second phases. With Zirconia as a second phase the major effect is the improvement of the composite thermal shock resistance [7]. The author concluded that the reinforcement was possible because of crack deviations and branching. A second attempt was made by Shi [8], who studied the influence of adding a 20 vol.% of stabilized Zirconia (Y-TZP) in a Zircon matrix; 40% toughness and a 20% strength increases were reported, the study showed that transformation and microcracking were the mechanisms involved in the increase of the toughness and strength. Zircon composites with SiC whiskers were processed and studied by Kondoh [9]; also better mechanical properties were achieved. Deng [10] showed that the addition of a 20 vol.% of SiC or TiC particles into a Zircon matrix, improves the crack propagation resistance. The influence of Mullite–Zirconia grains (MZ) on thermal shock resistance of Zircon based composites prepared by slip casting has been studied [11]. When MZ proportion is over 25 wt.% it cannot be considered as a simple additive. The addition of MZ provided an increase in the thermal shock resistance.

Usually in the case of dispersoidal composites, the Mullite component is used as a matrix [12–14]. But in the present work, the Mullite is incorporated in a wide range of compositions: from a reinforcement agent into a Zircon matrix to the Mullite matrix with dispersed Zircon grains proportions.

This kind of composites can be prepared by reaction sintering [15]. For this work the composites studied were obtained by direct sintering of Zircon and Mullite grains [16] because it is simple route, and a gradual change in the initial composition was correlated with a gradual change in the microstructural configuration. Simple sintering due to the action of temperature is expected and chemical transformations are intended to be avoided. Finally, if such a kind of sintering is achieved, the final microstructure would be of the same order than the starting powders dimension.

Thermomechanical properties of a similar reaction sintered Zircon–Mullite composites (≈17 wt.% Mullite) have been studied recently by Hamidouche et al. [15]. These authors concluded that the thermomechanical properties of the composite are situated in general between those of Mullite and those of Zircon when determined separately. The toughness and the fracture stress at room temperature of the composite were lower than those of the monolithic Zircon. At high temperature, the tendency was reversed. The elastic modulus remained always lower than those of the monolithic components whatever the temperature. Composite showed a combination of good mechanical strength as Zircon and suitable thermal shock resistance as Mullite materials.

The influence of the composition of Zircon–Mullite composites on the mechanical and fracture properties has been recently reported [16]. Reduction in the dynamic elastic modulus with the increasing added amount of Mullite was higher than that predicted from a mixing rule, probably due to the small residual porosity and the presence of microcracks resulting from the ZrO_2 transformation during the cooling. Fracture toughness and initiation energy increased with Mullite addition from which the Zirconia formation is enhanced. The toughness improvement was probably related to the increase in the total amount of Zirconia involving a microcracking mechanism rather than to a transformation toughening because the amount of t-ZrO_2, was low compared to the m-ZrO_2 content.

Zircon–Mullite composite materials do not escape to this issue because in the majority of its applications they are submitted to sudden changes of temperature, being in several cases its thermal shock resistance the usage limitation.

Theoretical TSR parameters R, R''' and R_{ST} are generally used to predict the thermal shock resistance of materials from their mechanical properties; these were calculated for the materials studied. A brief description of these parameters was included in following section. No important differences resulted from this classical analysis. Hence in this work both thermal shock resistance (TSR) and fatigue (TFR) of Zircon–Mullite composites with different compositions and microstructure configurations were experimentally evaluated by the non destructive measurement of the elastic modulus (E) and compared with the values of the theoretical parameters (R, R''' and R_{ST}) calculated from the experimental mechanical and fracture evaluation of these materials completed in a previous work [16]. Finally a simple mathematical modelling of the TFR data was also developed in this work in order to ease the data handling.

1.1. Theoretical thermal shock resistances parameters

The classical theoretical thermal shock resistance parameters for brittle material are derived from three theories or approximations, the thermoelastic approximation (TEA), an energy balance criteria (EBA) and finally a unified theory (UT) which contains the results of the other two and introduces a new parameter [17–20].

1.1.1. The thermoelastic approximation (TEA)

The thermoelastic approximation proposed by Kingery establishes that the fracture will occur when the thermal stress equals or overcomes the fracture strength of the material [18]. The R parameter is defined, for $h = \infty$ (h is the heat transfer coefficient):

$$R = \frac{\sigma_f(1-\nu)}{E\alpha} \quad (1)$$

where σ_f is the flexural strength, ν is the Poisson ratio; E is the elastic modulus and α is the thermal expansion coefficient. The R parameter is the critical thermal difference for the crack initiation ΔT_C.

1.1.2. The energy balance criteria (EBA)

The energy balance approximation was developed by Hasselman [17] and establishes that a sample will fracture if the thermoelastic energy is superior to the energy required for the creation of the crack surfaces, assuming that the only energy transferred is the elastic energy from the thermal stresses, the

following expression is deduced for the R''' parameter:

$$R''' = \frac{E}{\sigma_f^2(1-\nu)} \quad (2)$$

1.1.3. The unified theory (UT)

The unified theory of thermal shock fracture initiation and crack propagation in brittle materials [17,19] includes the parameters mentioned before, and defines a new parameter, the thermal stress crack stability parameter (R_{ST}). The R_{ST} parameter depends on the fracture surface energy (γ_i), the elastic modulus (E) and the linear thermal expansion coefficient (α). Once a crack has been initiated, thermal shock failure is controlled by the nature of the crack propagation through the material. This parameter can be used to predict the behaviour of materials with sufficiently long cracks under severe thermal stresses.

$$R_{ST} = \left[\frac{\gamma_i}{\alpha^2 E}\right]^{1/2} = \frac{K_{IC}}{\sqrt{2}\alpha E} \quad (3)$$

According to Hasselman [17] the first model is applicable to brittle materials where the crack initiation is determining in the behaviour. And the second approximation is valid where the initiation of the cracks is inevitable. In this work, the microstructure of the materials exhibited grains, pores, grain boundaries, microcracks as well as other defects which are unavoidable especially due to the processing method used. Thus it is expected that the TSR would be adequately predicted by the second approximation and the third theory.

1.2. Thermal shock evaluation

The TSR can be evaluated on heating or cooling, but in most methods a sudden cooling step is used because its greater severity. A usual method consists of heating the test probe to a desirable temperature followed by rapid cooling to room temperature (referred in this paper as the ''quenching'' method), by immersion in water. A characteristic mechanical property, related to the microstructure integrity, like fracture strength or elastic modulus is measured before and after quenching. The continuity and shape of the functionality (E vs. ΔT curve) depends on the microstructure of the material [21]. From this curve, the critical temperature differential (ΔT_C) can be evaluated. Composites with thermal cycles below ΔT_C do not suffer any damage because the elastic energies are less than the fracture energies required for the crack propagation. Above ΔT_C a marked E reduction will occur indicating that the thermal stress induced the appearance of new microcracks or propagated those ones originally present. This gradient (ΔT_C) is a typical TSR experimental parameter.

In service, refractory materials are not always submitted to a single thermal shock, which is the one that makes a certain piece fail; in fact the temperature changes are cyclic. In consequence it is of interest to evaluate the behaviour of a certain material after several thermal shock treatments. Thermal fatigue resistance evaluation (TFR) [22] consists in the measurement of a certain characteristic property of a material with successive thermal shock treatments. Both the experimental evidence and the theoretical models show certain saturation behaviour for the TFR of ceramic materials [23].

The effect of cracks and microcracks on the elastic modulus was reviewed by Stiffler and Hasselman [24]. Generally the resulting elastic modulus is a function of the number and lengths of the cracks, so the decrease in the elastic modulus after a thermal shock is directly related with the nucleation and propagation of the cracks in the material.

The elastic modulus (E) of a material, if the thermal shock treatment is severe enough, decreases in the first 3–5 cycles and then when the energy provided by the thermal shock is not high enough to propagate the existing cracks, the value of E does not change with the following thermal treatments; this stage is called the saturation stage.

To evaluate TSR and TFR behaviours an important number of probes and measurements have to be done especially if the characteristic property is evaluated by a destructive test like the bending test. Thus, other objective of this work is optimizing the number of measurements in order to fully describe the TFR; this was done by finding an empirical expression for describing this behaviour.

2. Experimental procedures

2.1. Slip casting of Zircon–Mullite composite materials

The processing of the materials was extensively described in [16]. In all the cases a commercial Zircon ($ZrSiO_4$) powder was used as principal raw material. With ZrO_2 = 64–65.5 wt.%, SiO_2 = 33–34 wt.%, $Fe_2O_3 \leq 0.10$ wt.% and $TiO_2 \leq 0.15$ wt.%. Mean diameter (D_{50}) of 1.5 μm. Specific gravity of 4.6 g/cm^3 and melting point of 2200 °C (Kreutzonit Super, Mahlwerke Kreutz, Germany).

A commercial Mullite powder was used as the second raw material. With Mullite 90–95 wt.%, glassy phase 5–10%, apparent density of 2.80 g/cm^3, true density of 3.13 g/cm^3, Al_2O_3 = 72%, SiO_2 = 20%, Fe_2O_3 = 0.2%, CaO–MgO = 0.3%, K_2O–Na_2O = 0.5%, mean diameter (D_{50}) of 2 μm (Synthetic Mullite M72, VAW, Veremigte, Werke AG, Germany).

Zircon and Mullite mixtures were prepared with 15, 25, 35 and 45 wt.% of Mullite and were called ZM15, ZM25, ZM35 and ZM45, respectively. The processing route chosen had been extensively explained in a previous work [14]. Aqueous 80 wt.% suspensions of the mixtures at pH 9.1–9.2 were prepared by adding the powder to aqueous solutions with suitable content of dispersant (Dolapix CE64, Zschimmers and Schwartz) and NH_4OH. After mixing, the suspensions were ultrasonicated for 20 min. The prismatic bars 7.5 mm × 7.5 mm × 50 mm were produced from well dispersed suspensions by slip casting in a plaster moulds. Dried probes were fired in an electric furnace with a heating rate of 10 °C/min up to 1600 °C for 2 h.

2.2. Characterization techniques

Density and open porosity of sintered samples were determined by the water absorption method. Theoretical density was calculated taking into account the density of each component: 3.16 g/cm^3 for Mullite and 4.56 g/cm^3 for Zircon. Crystalline phases formed were analyzed by X-ray diffraction (XRD) (Philips 3020 equipment with Cu-Kα radiation in Ni filter at 40 kV to 20 mA). The crystalline phases of the materials were quantified by the Rietveld method [25,26]. For the mechanical and fracture characterization prismatic bars of 7.5 mm × 7.5 mm × 50 mm were used. The dynamic elastic modulus E of the composites was measured by the excitation technique with a GrindoSonic, MK5 ''Industrial'' Model. Microstructural examination was conducted with a scanning electron microscope SEM (Quanta 200 MK2 Series de FEI) after polishing the probe surfaces until to 1 μm diamond paste. Flexural strength (σ_f) was measured on the bars with rectangular section using the three-point bending test with 40 mm of span and a displacement rate of 2.5 mm/min was employed (Universal testing machine INSTRON 4483). The fracture toughness (K_{IC}) and the fracture initiation energy (γ_i) were evaluated by the single edge notched beam method (SENB) [16,27] using a 3-point bending universal testing machine. Samples were notched with diamond saw of 0.3 mm thickness, with depth between 0.3 and 2.5 mm. The 3-point test was carried out at room temperature with a rate displacement of 0.1 mm/min.

2.3. The thermal shock behaviour testing

The evaluation of the thermal shock behaviour of the materials was carried out in two different experiments.

Firstly for the TSR experiments, the water quenching method was used. Thermal treatments with quenching temperature differentials, ΔT of 200, 400, 600, 800, 1000 and 1200 °C were applied. Five of the sintered prismatic samples were heated at a selected temperature in an electrical furnace in air atmosphere for a period of 30 min and then cooled in a water bath at 25 °C. After quenching, samples were dried at 100 °C and then the thermal shock effect on E was registered. The E/E_0 as a function of the temperature gradient curve is determined in the TSR experiment (where E and E_0 are the dynamic elastic modulus after and before the quenching test, respectively) and from which the experimental ΔT_C was evaluated.

For the TFR experiments also a repetitive water quenching method was used for a selected temperature differential (ΔT = 1000 °C), each cycle was carried out in the above-mentioned conditions. The dynamic elastic modulus was used to evaluate the microstructure degradation after the successive severe thermal cycles. The E/E_0 against number of cycles (N) graph is reported for the TFR experiment.

2.4. Materials properties

A Rietveld quantitative analysis was carried out to evaluate the present crystalline phases in the materials [25,26] (Table 1).

Table 1
Final composition of the Zircon–Mullite studied composites.

Material	Final crystalline phases[a] (wt.%)			
	Zircon	Mullite	ZrO_2 (total)	t-ZrO_2
ZM15	82	14	4	0.29
ZM25	73	23	4	0.35
ZM35	54	34	11	0.65
ZM45	46	44	10	0.75

[a] Evaluated by the Rietveld method from the XRD pattern.

The powder XRD patterns were analyzed with the program FullProf, which is a multipurpose profile-fitting program, including Rietveld refinement [28]. The starting crystallographic data for each phase were extracted from the literature. Finally taking into account that the amount of Zircon decreased in this series it is also obvious that the presence of Mullite increased both the decomposition of Zircon and the retention of the tetragonal Zirconia phase.

The sintered densities of the composites studied are shown in Table 2, composites presented a relative density of 91–92% of the theoretical one. Thus a similar porosity of around 8% was evidenced after sintering. Therefore all the materials showed to be relatively dense taking into account that they were processed by slip casting. The open porosity was ≤1.5% for all the studied composites, hence the sintering stage can be assumed to be equivalent for all the composites. Due to the difference in density of each phase is that the volume proportion of the components differs so much to the weight composition. The phase volume (V_i(%)) estimation was described in a previous work [16].

The mechanical and fracture characterization of the materials are shown in Table 3 and was extensively studied and described in a recent work [16]. Toughness and crack initiation surface energy increased with the amount of Mullite phase in the composite. The presence of Mullite decreased the value of E. Finally, the flexural strength of the composites (ZM15-45) decreased with the amount of Mullite.

SEM micrographs of the ZM15 and ZM45 materials are shown in Fig. 1. The samples had a dense microstructure with low residual porosity which is similar to that reported in previous works [11,15]. There is no a preferential direction in the microstructures of these materials. The microstructure of this materials obtained by slip casting of aqueous concentrated suspensions was similar to the one obtained by different processing methods.

Table 2
Texture properties and final volume composition of the Zircon–Mullite studied composites.

Material	Apparent density (g/cm^3)	Final crystalline phases (vol.%)		
		Zircon	Mullite	Zirconia (total)
ZM15	3.99	79.8	16.7	3.5
ZM25	3.85	69.6	27.0	3.4
ZM35	3.70	51.2	39.6	9.2
ZM45	3.55	42.2	49.6	8.2

Table 3
Mechanical and fracture properties of the Zircon–Mullite composites.

Material	E (GPa)	σ_f (MPa)	K_{IC} (MPa m$^{1/2}$)	γ_i (J/m^2)
ZM15	200 (±5)	142 (±10)	2.04 (±0.25)	10.3 (±3)
ZM25	191 (±5)	144 (±10)	2.08 (±0.25)	11.3 (±3)
ZM35	180 (±5)	128 (±10)	2.45(±0.25)	16.7 (±3)
ZM45	172 (±5)	131 (±10)	2.72 (±0.25)	21.4 (±3)

Table 4
Values of the theoretical TSR parameters of the studied materials.

Material	R (theoretical ΔT_C, °C)	R''' (MPa^{-1})	R_{ST}(m$^{1/2}$ °C)
ZM15	99	14.2	1.43
ZM25	106	13.1	1.54
ZM35	100	15.6	1.93
ZM45	106	14.3	2.23

Processed in the same conditions, composite materials (ZM15-45) show a high and similar degree of sinterization and low porosity. Different crystalline phases were observed and characterized by EDAX: dark grey grains of Mullite, middle grey grains of Zircon. In all the cases rounded Zirconia white grains can be observed as a product of the thermal decomposition of the Zircon. These are associated or near to the Zircon particles.

The two first composite ZM15 and ZM25 revealed a similar phase configuration, with a continuous Zircon matrix and well dispersed Mullite (5–10 μm) and Zirconia (1–2 μm) grains and corresponds to a Zircon–Mullite composite [16].

The volume percentage of Mullite (Table 2) of the ZM45 material is around 50%, this is concordant with the fact that in this case the phase configuration was opposite, there is a clear Mullite matrix with Zircon (5–10 μm) and Zirconia (≈2 μm) dispersed grains. This material should be classified as Mullite–Zircon composite material.

3. Results and discussion

3.1. Thermal shock resistance theoretical parameters

The theoretical parameters described above (Eqs. (1)–(3)) were calculated from the experimental mechanical and fracture properties of the materials (Table 3), and the values are shown in Table 4. The mechanical and fracture properties of Zircon and Mullite as unique phases are comparable, then it is expectable that composites with different proportions of these phases as principal constituents present similar mechanical and thermomechanical properties.

Particularly the mechanical properties of these materials depend on the phase composition and follow a kind of a mixing rule [16]. But the dependence of E and σ_f on Mullite content are parallel, therefore the E/σ_f ratio remained almost constant and compensated the TSR predictions from the TEA and EBA approximations (Eqs. (1) and (2)).

A contradiction is found from the parameters results. The first two parameters (R and R''') predict that TSR of these composites should be equivalent (values do not differ significantly) indicating a similar thermal shock behaviour for all the composites. On the other hand, the R_{ST} parameter predicts a clear improvement in the behaviour with the increase of the Mullite content in the composite. The higher value of this parameter observed for the 45 wt.% Mullite composite, anticipated a better behaviour. Consequently the need of an experimental examination was conclude in order to provide a confirmation of the predictions.

3.2. Experimental thermal shock resistance (TSR)

The microstructure degradation of the material was evaluated by a non destructive and dynamic method, the impulse excitation technique for testing the elastic modulus [29,30]. The results obtained by this method are comparable with the ones obtained by 3 or 4 points bending tests [31].

As mentioned previously, the presence of cracks and defects in the microstructure will decrease the value of E, therefore both the initiation and propagation of cracks will be followed

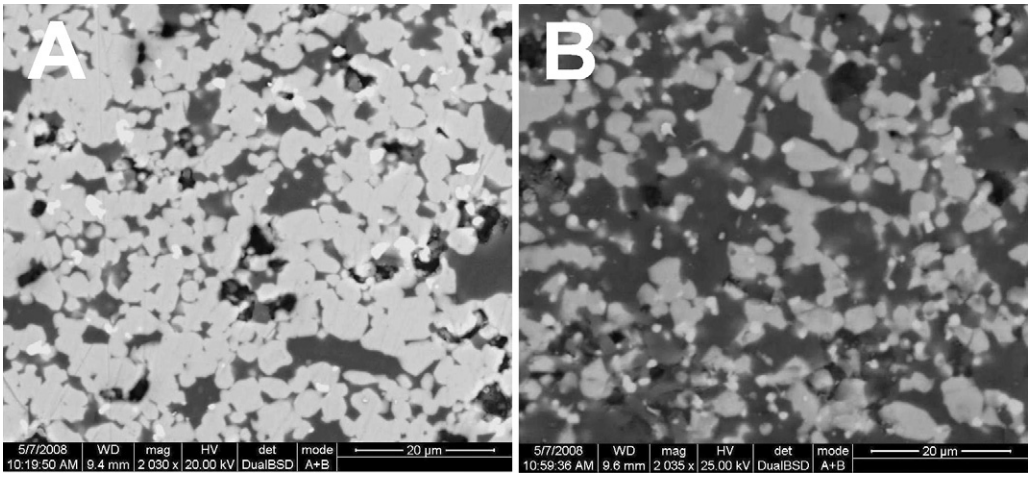

Fig. 1. Typical microstructure of the Zircon–Mullite materials ZM15 and ZM45 (A and B respectively).

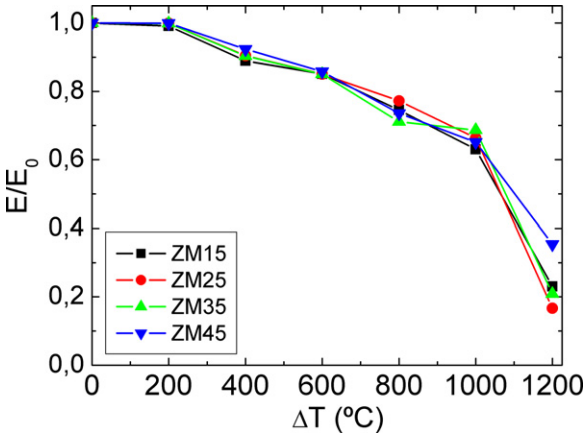

Fig. 2. TSR of the Zircon–Mullite composites.

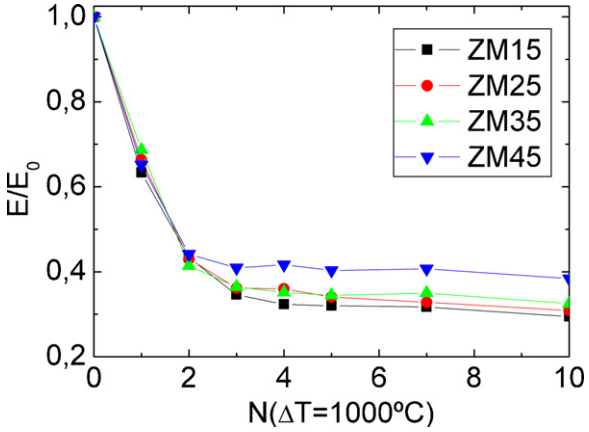

Fig. 3. TFR of the studied materials. $\Delta T = 1000\ ^{\circ}C$.

by this technique. In Fig. 2 the effect of the temperature gradient (ΔT) on E/E_0 is plotted. Following a classical analysis [18], the critical temperature gradient (ΔT_C) for all the materials was between 200 and 400 °C. In addition between ΔT_C and 1000 °C the decrease in the elastic modulus was constant and equivalent for the four composites up to $\Delta T = 1000\ ^{\circ}C$, retaining in this condition the 60% of the elastic modulus. Its important to point out that the microstructural configurations of this group of materials defers considerably (Fig. 1) moreover the continuous ceramic matrix changes from Zircon to Mullite; however the thermal shock resistance is equivalent up to this temperature (1000 °C).

With the most severe submitted thermal shock (1200 °C) the damage was more important; although the composites remained with no catastrophic damage, the Zircon–Mullite composites (ZM15, ZM25 and ZM35) lost the 80% of the dynamic elastic modulus evidencing an important damage after this treatment. With this level of severity the thermal shock resistance of the Mullite matrix material (Mullite–Zircon composite; ZM 45) was better, retaining almost the 40% of the original elastic modulus.

3.3. Thermal fatigue resistance (TFR)

Fig. 3 shows the relation E/E_0 (where E and E_0 are the dynamic elastic modulus after and before the quenching test respectively) as a function of the number of quenching tests of $\Delta T = 1000\ ^{\circ}C$ for the different compositions. As mentioned previously E decreased and corresponded to the microstructure degradation. For all the materials studied the TFR behaviour is similar to the reported in previous works for brittle solid materials and refractories [11,14,22,23]. An important decrease in the E/E_0 ratio after the second or third cycle is observed showing the microstructure was damaged. After that, with the successive thermal shocks the E value remained almost constant showing that there was no further damage, the development of the cracks stopped. The thermal energy from the thermal shock which is always the same is not high enough to propagate the great amount of cracks present in the microstructure.

The first three composites (ZM15-35) presented an equivalent behaviour retaining 35% of the elastic modulus. And no catastrophic damage was observed after ten cycles. Again the Mullite matrix composite (ZM45) presented a better behaviour in this case a superior TFR, retaining more than the 45% of the original elastic modulus. This material reached this saturation condition after the first two cycles while the other composites did it after three.

3.3.1. Mathematical modelling of the TFR

It is clear that the E/E_0 ratio should have a simple mathematical expression in terms of the number of quenching cycles (N).

$$\frac{E}{E_0} = F(N) \tag{4}$$

The curve proposed is an exponential decay with 3 parameters.

$$\frac{E}{E_0} = B + Ce^{(-bN)} \tag{5}$$

Taking into account the experimental conditions and the curve shape given by Eqs. (6) and (7).

$$Lim_{N\to\infty} F = \text{cte} = B \tag{6}$$

$$F(0) = 1 = B + C \tag{7}$$

Eq. (5) is simplified to Eq. (8) and the non exponential parameter is not independent, resulting in the thermal fatigue resistance expression for typical brittle materials evaluated by the elastic modulus:

$$\frac{E}{E_0} = B + (1 - B)e^{(-bN)} \tag{8}$$

where E and E_0 are the elastic modules after and before the quenching in water; N is the number of successive thermal treatments of $\Delta T = 1000\ ^{\circ}C$. Finally ($B$) and ($b$) are experimental parameters for TFR at 1000 °C which represents this behaviour. The parameter B is the final asymptotic or saturation value of E/E_0 named E_f/E_0. Moreover b is linked with the

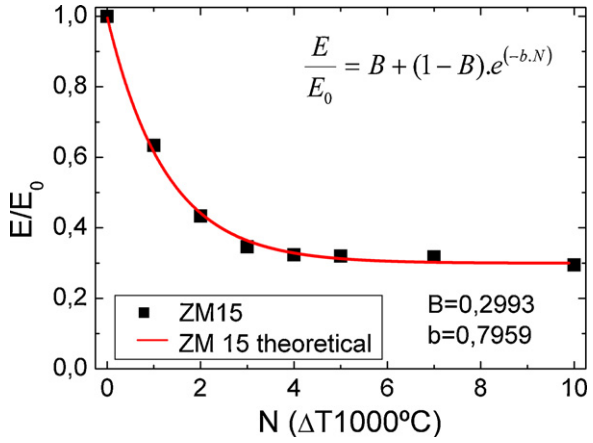

Fig. 4. Comparison between the experimental and theoretical TFR for the ZM15 composite with $\Delta T = 1000\ ^{\circ}C$.

initiation resistance of the material and B is related with the propagation allowed be the material with a certain thermal shock. A higher B and a lower b represent better thermal fatigue behaviours.

The experimental data for all the materials studied was fitted with this expression. In Fig. 4 the theoretical and experimental TFR of the ZM15 material are compared. The values for the different materials studied of B and b, resulting from the mean square analysis are shown in Table 5.

The difference between the calculated and the experimental data was always under 1%. The good fitting results with $R^2 \geq 0.99$ (Table 5) for all the materials indicates that the proposed equation was successfully used for characterizing the TFR of these materials. In order to extent this equation to several brittle materials, more materials should be analyzed, this is being carried out in our laboratory with satisfactory results, the outcome will be published in future publications.

The experimental parameters (b and B) evidenced that the behaviour of the first three composites materials are similar, and that the Mullite matrix composite material ZM45 presents a slightly better TFR. This together with the results obtained in Sections 3.2 and 3.3 show that this material (ZM45) presented better general thermal shock behaviour both TSR and TFR.

This could be related with the lower elastic modulus (E) and higher toughness (K_{IC}) and initiation fracture surface energy (γ_i) as a consequence of the higher Zircon dissociation and the microcracks developed by the dispersed m-ZrO_2 grains [16]. A clear indirect correlation between the elastic modulus and the B experimental TFR parameter is observed in Fig. 5A. Also a direct correlation between the fracture toughness and the same

Table 5
Values of the experimental TFR parameters of the studied materials.

Material	$\Delta T = 1000\ ^{\circ}C$		
	B_{1000}	b_{1000}	R^2
ZM15	0.29	0.78	0.996
ZM25	0.31	0.78	0.992
ZM35	0.32	0.79	0.982
ZM45	0.40	0.98	0.990

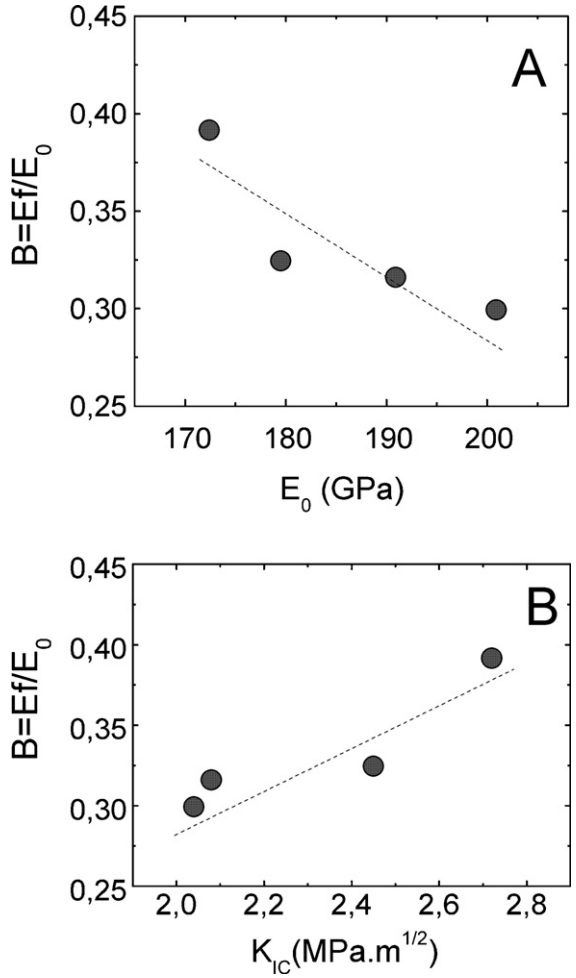

Fig. 5. Correlation between the thermal resistance saturation ratio (B) with: (A) the elastic modulus (E); (B) the fracture toughness.

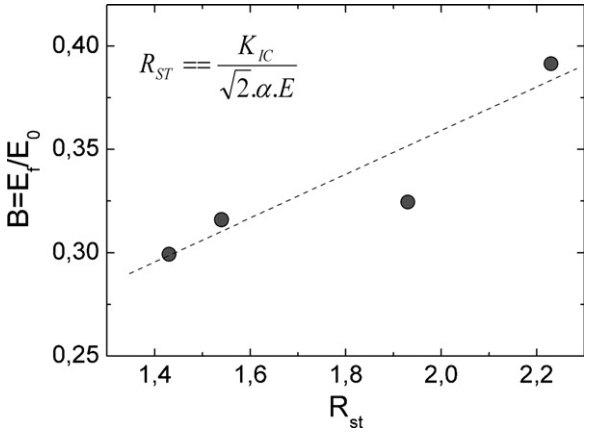

Fig. 6. Correlation between the thermal resistance saturation ratio (B) with the theoretical parameter R_{ST}.

experimental parameter is evident in Fig. 5B. In consequence, as shown in Fig. 6, the correlation between the experimental TFR and the R_{ST} taking into account the parameter definition showed Eq. (3) is expected assuming that the thermal expansion coefficient of these composites is invariant. This fact illustrates the merits of this parameter and particularly confirms

the benefit of the fracture toughness evaluation in the characterization of this kind of ceramic materials.

In a previous work [16] a clear correlation between the phase composition and the mechanical and fracture behaviour of these composites was shown, in the present work the relation between the mechanical and fracture properties and the thermal shock behaviour was established showing that the three are strongly related.

4. Conclusions

In a previous work [16] a clear correlation between the phase composition and the mechanical and fracture behaviour of these composite was revealed. In the in present study the relation between the mechanical and fracture properties and the thermal shock behaviour was established showing that the three (composition-mechanical and fracture properties-thermal shock behaviour) are strongly related.

Both the TSR and TFR of slip cast Zircon–Mullite and Mullite–Zircon composite materials were evaluated by a dynamic elastic modulus measurement. All the materials studied showed typical brittle behaviours with similar ΔT_C between 200 and 400 °C.

A mathematical modelling of the TFR experimental data permitted to do a comparison of the materials and contrast them with the outcome of the theoretical analysis. This was achieved with a simple empirical expression with very good agreement between the calculated and the experimental data. From which an experimental thermal fatigue parameter (B) was derived which is the saturation value of the elastic modulus ratio (E_f/E_0). Higher value of B parameter indicates an improvement in the TFR. The B parameter of this series of composites slightly increased with the Mullite content.

Although the microstructural configurations studied differed considerably, the experimental behaviour of this group of materials was similar. This fact was satisfactorily predicted by the theoretical parameters (R and R''') showing the importance of the mechanical evaluation of the ceramic material, that define these two parameters. On the other hand the slight difference evaluated in the TFR was correlated with the only parameter that takes into account the fracture toughness (R_{ST}) showing that the significance of this property in a more deep characterization of the ceramic materials.

References

[1] A. Everett, T. Thomas, T. Weichert, Trends in usage in glass industry, in: Proc.: UNITECR, 1989, 730–760.

[2] J. Mori, N. Watanbe, M. Yoshimura, Y. Oguchi, T. Kawakami, A. Matsuo, Materials design of monolithic refractories for steel ladle, in: Proc.: UNITECR, 1989, 541–553.

[3] L.B. Garrido, E.F. Aglietti, Zircon based ceramics by colloidal processing, Ceram. Int. 5 (2001) 491–499.

[4] A. Kaiser, M. Lobert, R. Telle, Thermal stability of zircon ($ZrSiO_4$), J. Eur. Ceram. Soc. 28 (11) (2008) 2199–2211.

[5] R.S. Pavlik, H.J. Holland, E.A. Payzant, Thermal decomposition of zircon refractories, J. Am. Ceram. Soc. 84 (12) (2001) 2930–2936.

[6] H. Schneider, J. Schreuer, B. Hildmann, Structure and properties of Mullite—a review, J. Eur. Ceram. Soc. 28 (2008) 329–344.

[7] R.C. Garvie, Improved thermal shock resistant refractories from plasma dissociated zircon, J. Mater. Sci. 14 (1979) 817–825.

[8] Y. Shi, Synergistic strengthening and toughening of zircon ceramics by addition of SiC whiskers and 3Y-TZP simultaneously, J. Eur. Ceram. Soc. 17 (1997) 1003–1010.

[9] I. Kondoh, Sintering of zircon–silicon carbide whiskers composites and their mechanical properties, J. Eur. Ceram. Soc. 101 (1993) 358–361.

[10] Z.-Y. Deng, Effect of residual stress on R-curve behaviour of ceramic matrix composites, J. Mater. Sci. Lett. 16 (1997) 977–981.

[11] N.M. Rendtorff, L.B. Garrido, E.F. Aglietti, Effect of the addition of Mullite–Zirconia to the thermal shock behavior of zircon materials, Mater. Sci. Eng. A 498 (s1–2), International Conference on Recent Advances in Composite Materials (ICRACM 2007) 208–215 (2008).

[12] M. Hamidouche, N. Bouaouadja, H. Osmani, R. Torrecillas, G. Fantozzi, Thermomechanical behaviour of mullite zirconia composite, J. Eur. Ceram. Soc. 16 (1996) 441–445.

[13] D. Kaberi, G. Banerjee, Mechanical properties and microstructures of reaction sintered mullite–zirconia composites in the presence of an additive-disprosia, J. Eur. Ceram. Soc. 20 (2000) 153–157.

[14] N.M. Rendtorff, L.B. Garrido, E.F. Aglietti, Thermal shock behavior of dense mullite–zirconia composites obtained by two processing routes, Ceram. Int. 34 (8) (2008) 2017–2024.

[15] M. Hamidouche, N. Bouaouadja, R. Torrecillas, G. Fantozzi, Thermo-mechanical behavior of a zircon–mullite composite, Ceram. Int. 33 (4) (2007) 655–662.

[16] N.M. Rendtorff, L.B. Garrido, E.F. Aglietti, Mechanical and fracture properties of zircon–mullite composites obtained by direct sintering, Ceram. Int. 35 (7) (2009) 2907–2913.

[17] D.P.H. Hasselman, Unified theory of thermal shock fracture initiation and crack propagation in brittle ceramics, J. Am. Ceram. Soc. 52 (11) (1969) 600–604.

[18] C. Baudin, Resistencia de los refractarios al choque térmico I, Boletín de la Sociedad Española de Cerámica y Vidrio 32 (4) (1993) 237–244.

[19] C. Baudin, Resistencia de los refractarios al choque térmico II, Boletín de la Sociedad Española de Cerámica y Vidrio 32 (5) (1993) 293–298.

[20] D.P.H. Hasselman, Elastic energy at fracture and surface energy as design criteria for thermal shock, J. Am. Ceram. Soc. 46 (1963) 535–540.

[21] B. Cotterel, W.O. Sze, Q. Caidong, Thermal shock and size effects in castable refractories, J. Am. Ceram. Soc. 78 (8) (1995) 2056–2064.

[22] S. Niyogi, A. Das, Prediction of thermal shock behaviour of castable refractories by sonic measurements, Interceram 43 (6) (1994) 453–457.

[23] V.R. Vedula, D.J. Green, J.R. Hellmann, A.E. Segall, Test methodology for the thermal shock characterization of ceramics, J. Mater. Sci. 33 (22) (1998) 5427–5432.

[24] R.C. Stiffler, D.P.H. Hasselman, Shear moduli of composites with elliptical inclusions, J. Am. Ceram. Soc. 66 (3) (1983) C52–C53.

[25] H.M. Rietveld, A profile refinement method for nuclear and magnetic structures, J. Appl. Cryst. 2 (1969) 65–71.

[26] D.L. Bish, J.E. Post, Quantitative mineralogical analysis using the Rietveld full-pattern fitting method, Am. Miner. 78 (1993) 932–940.

[27] J. Kübler, Fracture toughness of ceramic using the SEVNB method: preliminary results, Ceram. Eng. Sci. Proc. 18 (4) (1997) 155–162.

[28] J. Rodríguez-Carbajal, Program FullProf. 98, version 0.2, (1998).

[29] ASTM C1548 – 02(2007), Standard test method for dynamic Young's Modulus, shear modulus, and Poisson's ratio of refractory materials by impulse excitation of vibration (2007).

[30] ASTM C1259 – 08(2008), Standard test method for dynamic Young's modulus, shear modulus, and Poisson's ratio for advanced ceramics by impulse excitation of vibration (2008).

[31] M. Radovic, E. Lara-Curzio, L. Riester, Comparison of different experimental techniques for determination of elastic properties of solids, Mater. Sci. Eng. A 368 (1–2) (2004) 56–70.